FEBS Letters

FEBS PRESS science publishing by scientists

Identification and functional characterization of a bacterial homologue of Zeta toxin in *Leishmania donovani*

Akriti Srivastava[1], Swati Garg[1], Ravi Jain[1], Rajagopal Ayana[1], Himani Kaushik[2], Lalit Garg[2], Soumya Pati[1] and Shailja Singh[1,3]

1 Department of Life Sciences, School of Natural Sciences, Shiv Nadar University, Greater Noida, India
2 Gene Regulation Laboratory, National Institute of Immunology, New Delhi, India
3 Special Centre for Molecular Medicine, Jawaharlal Nehru University, New Delhi, India

Correspondence
S. Singh, Special Centre for Molecular Medicine, Jawaharlal Nehru University, New Delhi, India
Tel: +91-11-2670-4559 Ext-303
E-mail: shailja.jnu@gmail.com

Swati Garg, Ravi Jain and Rajagopal Ayana have equal contribution

(Received 5 February 2019, revised 5 March 2019, accepted 11 March 2019, available online 24 May 2019)

doi:10.1002/1873-3468.13429

Edited by Renee Tsolis

Zeta-toxin is a cognate toxin of epsilon antitoxin of prokaryotic Type II toxin-antitoxin system (TA) and play an important role in cell death. An orthologue of bacterial-zeta-toxin (BzT) was identified in *Leishmania donovani* with similar structural and functional features. *Leishmania* zeta-toxin (named Ld_ζ1) harboring similar UNAG and ATP-binding pockets showed UNAG kinase and ATP-binding activity. An active Ld_ζ1 was found to express in infective extracellular promastigotes stage of *L. donovani* and episomal overexpression of an active Ld_ζ1domain-triggered cell death. This study demonstrates the presence of prokaryotic-like-zeta-toxin in eukaryotic parasite *Leishmania* and its association with cell death. Conceivably, phosphorylated UNAG or analogues, the biochemical mimics of zeta-toxin function mediating cell death can act as a novel anti-leishmanial chemotherapeutics.

Keywords: anti-leishmanial; autophosphorylation; cell death; *L. donovani*; UNAG kinase activity; zeta toxin

Leishmania is a trypanosomatid parasitic protozoan responsible for one of the most neglected tropical human disease, leishmaniasis. *Leishmania* parasites are dimorphic and hence adapt and develop in an insect vector and a vertebrate host to complete their life cycle. It has two forms, one is promastigote that resides extracellularly in the sand-fly alimentary tract, and the other is amastigote that exists intracellularly in the parasitophorous vacuole of human macrophages, dendritic cells, and fibroblasts [1]. Leishmaniasis is caused by nearly 20 *Leishmania* spp. that are transmitted to humans by more than 30 different species of infected female phlebotomine sand flies [2]. The complexity of the disease is mainly attributed to species diversity of vectors and parasites involved in the pathogenesis. Visceral leishmaniasis (VL), caused by *Leishmania donovani* and *Leishmania infantum*, is the most severe form, which is characterized by irregular bouts of fever, weight loss, anemia and enlargement of the spleen and liver, along with death in chronic cases. The global epidemic graph of VL reported emergence of an estimated 50 000 to 90 000 new cases each year as depicted by WHO, 2015 [http://www.who.int/news-room/fact-sheets/detail/leishmaniasis]. Although VL is not rated high in global burden of diseases, yet it is becoming a cause of concern due to high-fatality, HIV co-infection and absence of vaccine [3,4]. In addition, frontline drugs available against VL exhibit limitations like limited efficacy, toxicity, difficult dosing regimens, and emerging resistance [5].

Abbreviations
BzT, bacterial-zeta-toxin; CFU, colony forming unit; CLAR, Central Laboratory Animal Resources; GPI, Glycosylphosphotidylinositol; JNU, Jawaharlal Nehru University; LB, Luria-Bertani; PI, Propidium Iodide; UNAG, Uridine diphosphate N-acetyl glucosamine; VL, visceral leishmaniasis.

Availability of the sequenced *L. donovani* genome [6] is a silver lining for the identification of new targets and development of novel chemotherapeutics. Over the last decade, several approaches have been used at genomic, transcriptomic, and proteomic levels to recognize new targets from pathways that are crucial to the pathogen but prominently distinct or absent in human. As *Leishmania* is a primitive eukaryote, it is known to exhibit some prokaryotic characteristics as well, such as polycistronic transcription [7]. Similarly, it may have some survival adaptation patterns of prokaryotes, which can provide new insights into a milestone approach for target identification. The Zeta toxin of Type-II Toxin-Antitoxin (TA) system of prokaryotes is one such protein that is putatively found in most of the kinetoplastids based on available genome sequences (http://tritrypdb.org/tritrypdb/).

TA system loci of prokaryotes are bicistronic operons that encodes for stable proteinaceous toxin and unstable neutralizing protein or small RNA as antitoxin. Existence of these systems was earlier reported as episomal genetic elements meant to enhance plasmid stability by postsegregational killing, but later their presence was also detected on chromosomes for preservation of transposable elements [8,9]. Additional functions assigned to TA module include prevalence of persister cells, stress response, protection from phage, regulation of biofilm formation, and virulence. Toxin and antitoxin usually forms complex and thus, antitoxin neutralizes the toxic activity of toxin. Under certain adverse circumstances, TA balance disrupts and labile antitoxin is degraded allowing the free toxin to inhibit several cellular processes such as translation, replication, ATP synthesis, cytoskeleton polymerization, and peptidoglycan synthesis [9–11].

Depending on the nature and the mode of inhibition by antitoxin, TA systems are classified into six different types. Type I and Type III features sRNA as antitoxin whereas Type II, IV, V, and VI are characterized by protein as antitoxin [12,13].

Both toxin and antitoxin of Type II TA system exists as protein and binding with antitoxin results in structural changes in toxin, thus blocking the catalytic sites for its action [14]. Rel B and zeta toxin are the most widely spread Type II toxins in prokaryotes [15]. Binding of antitoxin epsilon to zeta toxin neutralizes its toxicity. Structurally, the zeta toxin folds like a phosphotransferase with Walker-A motif in the center, responsible for ATP binding [16,17]. Notably, in case of bacterial peptidoglycan synthesis, MurA enzyme catalyzes the transfer of the enolpyruvyl moiety of phosphoenolpyruvate to the 3′-hydroxyl group of Uridine diphosphate N-acetyl glucosamine (UNAG), finally yielding enolpyruvyl-UNAG via formation of tetrahedral intermediate [18,19]. However, in the presence of zeta toxin, UNAG gets phosphorylated to UNAG-3P via ATP hydrolysis, which then binds to MurA and blocks its catalytic activity. This leads to the blockage of peptidoglycan synthesis pathway, resulting in autolysis of cells [20]. Remarkably, based on environmental condition and dose of zeta toxin, cells may either undergo postsegregational killing or cell stasis [21,22]. Intriguingly, zeta toxin from *N. gonorrhoeae* phosphorylates the multiple UDP-activated sugar substrates, making them unavailable for binding to MurA, MurB, MurC, leading to abrogated cell wall synthesis [23].

Although, zeta toxin has a remarkable role in prokaryotic pathogenicity, its occurrence in eukaryotic parasites is unexplored till date. Putative appearance of zeta toxin homologues in all the kinetoplastides prompted us to examine the relevance of this protein in trypanosomatids. We describe here the existence of zeta toxin like protein in *L. donovani* (Ld_ζ1) and its characterization in promastigotes and heterologous prokaryotic system *Escherichia coli*. We could show that recombinant zeta toxin domain from *L. donovani* ($Ld\_\zeta1_{domain}$), similar to prokaryotic zeta toxin has UNAG kinase activity and its expression shows toxic effect in *E. coli* as a repercussion of damaged cell wall. It also shares similar UNAG-binding pocket residues, as earlier shown in canonical zeta toxins. However, in contrast to the known zeta toxins, $Ld\_\zeta1_{domain}$ showed autophosphorylation that is the characteristic of eukaryotic kinases. Further, we had overexpressed GFP tagged $Ld\_\zeta1_{domain}$ in *L. donovani* promastigotes and observed similar phenotype as in *E. coli* heterologous expression system. To highlight, homologue of zeta toxin has not yet been reported in eukaryotes, thus Ld_ζ1 is the first described parasitic zeta toxin having UNAG kinase activity and unique autophosphorylation activity.

Materials and methods

Bacterial strains, plasmids and reagents

The *E. coli* strains used in this work are DH5α, BL21 (λDE3), and BL21-CodonPlus harboring pET-22b(+) plasmid fused with $Ld\_\zeta1_{domain}$ insert. The strains were grown in liquid or solid Luria-Bertani (LB) medium with 100 $\mu g \cdot mL^{-1}$ of ampicillin at 37 °C, if not mentioned otherwise. PCR reagents, DNA-modifying enzymes, and kits for molecular biology experiments were obtained from Thermo Fisher Scientific (Haryana, India). All enzymes were used as recommended by the supplier. The

oligonucleotide primers used in this study were obtained from Sigma-Aldrich (New Delhi, India). Primer Sequence used for amplifying Ld_ζ1 by semi-quantitative PCR is as follows: Forward primer (TGTCGTGAATGCCGATGAGT) and Reverse primer (CGACAACCTGCTGCACAAAC).

In vitro culture of *Leishmania donovani*

The *L. donovani* promastigote were adapted at 26 °C in M199 medium, pH 7.5 supplemented with 10% heat inactivated FBS and the culture density was maintained at 2×10^6/mL. Promastigotes. Whole cell lysate of Promastigote was prepared by freeze–thaw cycles as described previously [24].

In silico search for Zeta toxin like protein in *Leishmania donovani*

The kinetoplastid database TriTrypDB (www.tritrypdb.org) was explored extensively for the presence of any homologue of prokaryotic zeta toxin in *L. donovani*. Sequence alignments and identity calculations were performed in ClustalW. Phylogenetic tree analysis of homologues of zeta-like proteins from kinetoplastids as well as prokaryotes was performed using publicly available Molecular Evolutionary Genetics Analysis (MEGA7) tool and the evolutionary history was inferred using the Neighbor Joining method. The bootstrap consensus tree inferred from 800 replicates and the evolutionary distances were computed using the Poisson correction method. 1GVN was taken as template for Homology modeling of Ld_$\zeta1_{domain}$ by Modeller software. Binding affinity of substrate UNAG and ATP to Ld_$\zeta1_{domain}$ was determined as described previously [25]. Briefly, Autodock vina and Autodocktools were used to prepare the protein and ligand structures for facilitating molecular docking.

Cloning, expression, purification and generation of anti-sera against Ld_$\zeta1_{domain}$

the primers used for cloning of Ld_ζ1domain were designed based on the *L. donovani* genome sequence. Ld_$\zeta1_{domain}$ was cloned in pET-22b(+) (6x-His tag at C-terminus) vector. Overexpression of Ld_$\zeta1_{domain}$ in *E. coli* BL21 (λDE3) was induced by addition of 1 mM IPTG at an OD_{600} of 0.6 and further incubated at 37 °C for 6 h. Cells were harvested by centrifugation, resuspended in Buffer A (10 mM Tris, pH 8) and lysed by sonication. Cell debris was cleared by centrifugation and the obtained pellet was solubilized in 8 M urea. The solubilized protein was collected by centrifugation and the supernatant was loaded on 1 mL Nickel Affinity resin (Qiagen) equilibrated with Buffer A. After washing with 30 mL of Buffer A, bound proteins were eluted with Buffer B (Buffer A supplemented with 8 M Urea and 250 mM Imidazole). Denatured protein thus obtained was refolded by slow pulsatile dilution in Buffer C (10% sucrose in Buffer A). Subsequent to overnight dialysis against 1 l of Buffer C, the protein was concentrated by using 3 kDa centricon (Merck Millipore, Mumbai, India).

A group of five Balb/c mice was immunized intraperitoneally. Before injecting the antigen, a preimmune serum was collected. For immunization, 25 μg purified protein emulsified with complete Freund's adjuvant; CFA (Sigma-Aldrich) was immunized on day 0 followed by two boosts emulsified with incomplete Freund's adjuvant on days 21 and 42. After the 42nd day, mice bleed was collected and serum was harvested. Animal experiments were conducted at Central Laboratory Animal Resources (CLAR), Jawaharlal Nehru University (JNU), New Delhi, India. Care and handling of experimental animals was in accordance with the Institutional Animal Ethics Committee (IAEC) of JNU.

In vitro kinase assay

The *in vitro* kinase activity of Ld_$\zeta1_{domain}$ was investigated as previously described [20] with slight modification. Briefly, 2 μM of rZeta was set for reaction in reaction buffer (25 mM HEPES-NaOH, pH 7.5; 100 mM NaCl and 5 mM $MgCl_2$) with 2 mM UNAG in presence of 1 μM ATP. The reaction was incubated at 25 °C for 1 h. After incubation, kinase activity was measured by utilizing ADP-Glo™ Kinase assay (Cat. no. V6930). This assay system involves ATP regeneration-based luciferase reaction system resulting from nascent ADP phosphorylation. The luminescence signal generated is proportional to the amount of ADP released in the kinase reaction and represents the kinase activity.

Interaction of rZeta with ATP by surface plasma resonance

To investigate the interaction of Ld_$\zeta1_{domain}$ with ATP, Ld_$\zeta1_{domain}$ protein was immobilized on a gold chip and association constant for interaction was calculated using the instrument Autolab ESPRIT. Before immobilization of enzyme Ld_$\zeta1_{domain}$, the gold chip was activated by injecting the 50 μL of 1 : 1 mixture of EDC (400 mM) and NHS (100 mM) over the chip surface followed by immediate injection of 100 μL enzyme (0.5 $mg{\cdot}mL^{-1}$ in 10 mM HEPES and 150 mM NaCl) in channel 2 of the instrument. Gold chips immobilized with the enzyme were blocked in order to avoid nonspecific binding of antigen over the immobilized surface during sensing process. For negative control, the enzyme was immobilized in channel 1 and 10 mM HEPES (pH-7.4) was injected (without substrate). Affinity measurement and detection limit were studied for varying concentrations of ATP, prepared in 10 mM HEPES and injected in channel 2 only. Association and dissociation

were performed for 300s and 150s, respectively. Subsequently, 50 mM NaOH was used to achieve regeneration of the sensor surface after each interaction and Ld_ζ1$_{domain}$ was recovered in order to bring the signal back to the baseline level so as to start a new cycle.

Evaluation of growth rate and toxicity in *Escherichia coli*

Toxicity of Ld_ζ1$_{domain}$ in *E. coli* BL21 (λDE3) was determined by monitoring the growth rate of *E. coli* BL21-CodonPlus overexpressing Ld_ζ1$_{domain}$ in the presence and absence of 1 mM IPTG. Overnight grown bacterial culture was subcultured to an OD_{600} of 0.07 and Overexpression of Ld_ζ1$_{domain}$ was induced at 37 °C, 25 °C, and 18 °C. Cell proliferation was monitored by measuring absorbance at 600 nm after every 2 h for 12 h.

To study toxic activity of Ld_ζ1$_{domain}$, a culture of *E. coli* BL21-CodonPlus with plasmid expressing pET22b(Ld_ζ1$_{domain}$) was grown to OD_{600} = 0.07 at 37 °C. Protein expression was induced with IPTG along with addition of 2 mM UNAG to induced and uninduced cultures, after which the incubation temperature was reduced to 18 °C. For CFU experiment on solid media, the culture was diluted to 10^{-1}, 10^{-3}, 10^{-5} and 10^{-6}, and 5 μL of different dilutions were spread on LB agar and plate was incubated at 37 °C.

Fluorescence microscopy

Staining of live/dead cells was performed using Hoechst and Propidium Iodide (PI). Hoechst is a nuclei staining dye that allows staining of viable cells, whereas, PI cannot cross the membrane of live cells making it useful to differentiate 'membrane-compromised' dead cells. A quantity of 500 μL of cell suspension was harvested by centrifugation, washed to remove residual media and stained with Hoechst, which stains all viable cells blue, and PI, which stains membrane-compromised cells red, according to the manufacturer's instructions (Thermo Fisher Scientific Cat. no. P3566). Hoechst positive cells were visualized with a 350 nm excitation filter and a 461 nm long pass emission filter, while propidium iodide-positive dead cells were visualized using a 545 nm band pass excitation filter and a 590 nm long pass emission filter.

Immunoblotting

Total protein extract was prepared from promastigotes at stationary growth phase of *L. donovani*. Cell lysate was obtained by direct lysis in the sample buffer (0.12 M Tris-HCl, pH 6.8; 4% SDS; 20% glycerol, and 10% 2-mercaptoethanol). After electrophoresis of lysate on SDS/PAGE (8%), proteins were transferred onto the PVDF membrane. Membrane-bound proteins were probed with anti-Ld_ζ1$_{domain}$ mouse sera diluted to 1 : 800 followed by probing with HRP conjugated rabbit anti-mouse IgG antibody, diluted to 1 : 10 000.

Immunofluorescence assay

For the intracellular localization of Ld_ζ, promastigotes were immobilized on poly-L-lysine-coated coverslips. The cells were fixed and permeabilized followed by incubation with the anti-Ld_ζ1$_{domain}$ mouse sera (1 : 500) for 1 h at RT. Subsequently, the cells were washed and then incubated for 45 min with the Alexa 488-conjugated Goat anti-mice (H+L) IgG antibody (Thermo Fisher Scientific). The nuclear and kinetoplastid DNA were stained with DAPI (Thermo Fisher Scientific). Immunofluorescence staining of parasites was visualized under fluorescence microscope (Nikon, Towa Optics (I) Pvt Ltd., New Delhi, India).

Results and discussion

Genome Analysis of *Leishmania donovani* revealed a novel Zeta toxin like protein (Ld_ζ1)

Zeta toxins, categorized under Type-II toxin-antitoxin system are yet to be fully explored in eukaryotes. Toward this, we extensively explored *L. donovani* genome database and came across three variants of Zeta toxin like protein, based on signature domain (zeta), such as zeta like protein 1, zeta like protein 2, and zeta like protein 3.

The prokaryotic zeta toxins are comprised of Walker-A motif containing P-loop (GXXXXGKT/S) for binding to ATP and Walker-B motif followed by a short consensus sequence GTXR that form a UNAG binding cleft [26]. Zeta toxin like protein 1

Fig. 1. Genome Analysis of *L. donovani* revealed a novel Zeta toxin like protein (Ld_ζ1). (A) Gene structure of Zeta toxin like protein 1 in *L. donovani*. (B) Sequence Alignment of Ld_ζ1$_{domain}$ from kinetoplastids and zeta toxin from prokaryotes. Conserved Walker-A motif, required for ATP binding is marked as green block. Motif that forms contact with UNAG is marked as orange block. (C) Ld_ζ1$_{domain}$ (black) was superimposed with zeta toxin of *S. pyogenes* (gray, PDB ID- 1GVN). Walker-A motif for ATP binding in Ld_ζ1$_{domain}$ (green) and 1GVN (red) superimpose well. UNAG-binding region of Ld_ζ1$_{domain}$ (orange) is also overlapping with 1GVN UNAG motif (red). (D) Phylogenetic relationship of Ld_ζ1$_{domain}$ with other zeta toxin like protein1 of kinetoplastids and zeta toxin of prokaryotes mentioned in multiple sequence alignment. Bootstrap values with 800 replicates with the neighbor joining method using MEGA 7.0. ▲ denotes kinetoplastids while ◆ denotes prokaryotes. (E) Ld_ζ1$_{domain}$ predicted model bound to ATP and UNAG at their respective clefts. Probable residues important for ATP and UNAG binding are shown in inset as stick model. Red region represents Walker-A motif.

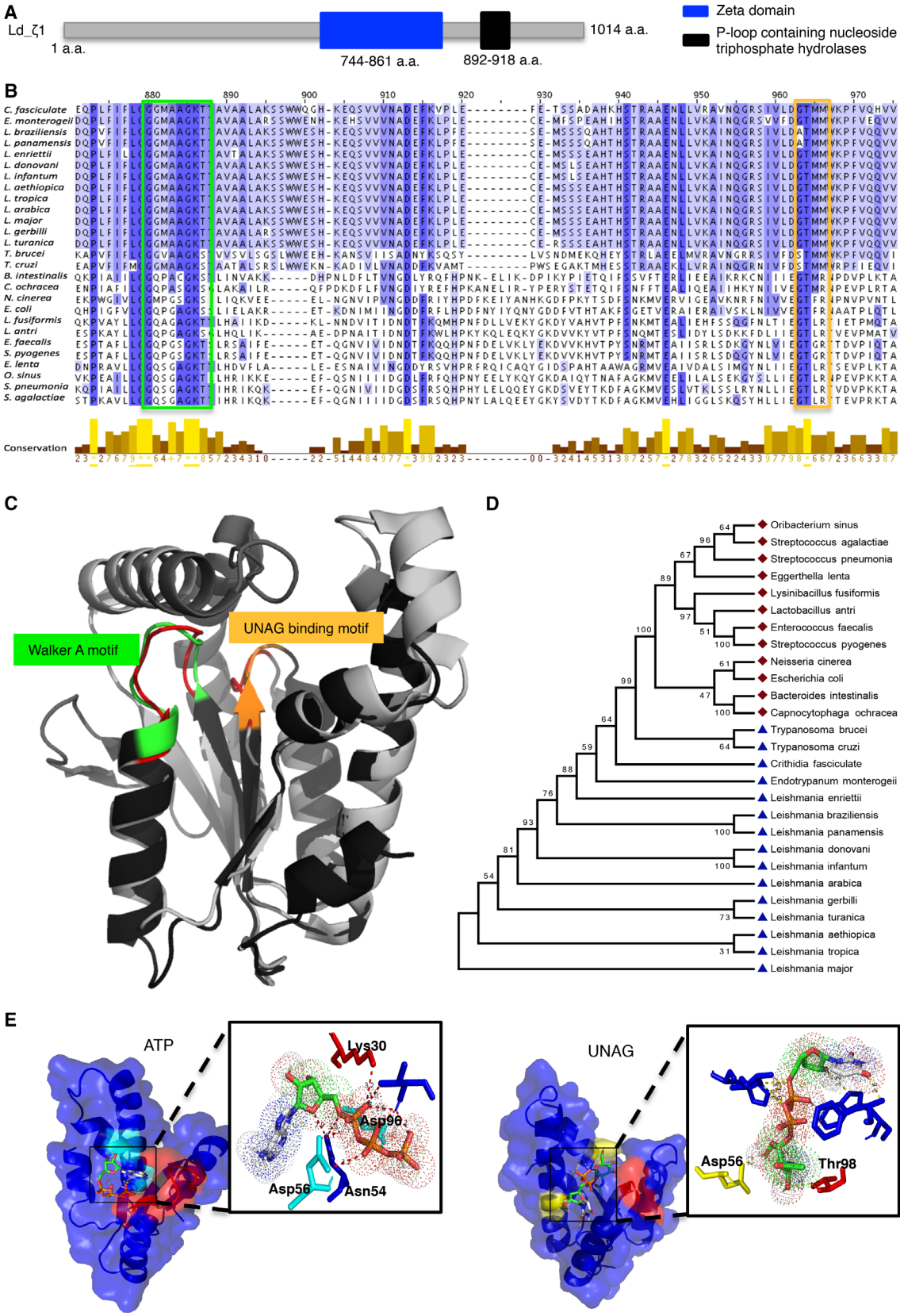
A
Ld_ζ1
1 a.a.
744-861 a.a.
892-918 a.a.
1014 a.a.
Zeta domain
P-loop containing nucleoside triphosphate hydrolases
B
C. fasciculate
E. monterogeii
L. braziliensis
L. panamensis
L. enrietti
L. donovani
L. infantum
L. aethiopica
L. tropica
L. arabica
L. major
L. gerbilli
L. turanica
T. brucei
T. cruzi
B. intestinalis
C. ochracea
N. cinerea
E. coli
L. fusiformis
L. antri
E. faecalis
S. pyogenes
E. lenta
O. sinus
S. pneumonia
S. agalactiae
Conservation
C
Walker A motif
UNAG binding motif
D
Oribacterium sinus
Streptococcus agalactiae
Streptococcus pneumonia
Eggerthella lenta
Lysinibacillus fusiformis
Lactobacillus antri
Enterococcus faecalis
Streptococcus pyogenes
Neisseria cinerea
Escherichia coli
Bacteroides intestinalis
Capnocytophaga ochracea
Trypanosoma brucei
Trypanosoma cruzi
Crithidia fasciculate
Endotrypanum monterogeii
Leishmania enrietti
Leishmania braziliensis
Leishmania panamensis
Leishmania donovani
Leishmania infantum
Leishmania arabica
Leishmania gerbilli
Leishmania turanica
Leishmania aethiopica
Leishmania tropica
Leishmania major
E
ATP
Lys30
Asp96
Asp56
Asn54
UNAG
Asp56
Thr98

(LdBPK_341740.1) is a 1014 amino acid protein (~111.5 kDa) that contains zeta domain (118 aa) and P-loop containing nucleoside triphosphate hydrolase domain, similar to the bacterial homologue. Unlike prokaryotes, Ld_ζ1 does not appear to constitute a classical epsilon/zeta TA system. Instead, the Ld_ζ1 protein sequence consists of a 743 aa long N-terminus, 118 aa long zeta domain in the center and a short 153 aa C-terminus. A schematic representation of the Ld_ζ1 protein is depicted in Fig. 1A. In addition, putative homologues of Ld_ζ1 are present in all kinetoplastids with some variations in their sequences. An alignment of the predicted protein sequences of these putative zeta toxin genes in kinetoplastid show that similar to prokaryotic zeta toxin, Ld_ζ1$_{domain}$ has both Walker-A and Walker-B motif but in GTXR consensus motif, R is replaced by M and is conserved throughout the kinetoplastid (Fig. 1B).

To understand the evolutionary relationships between prokaryotic zeta toxins and putative orthologues in other kinetoplastids, we constructed a phylogenetic tree via the Neighbor Joining method. The protein sequences of the individual kinetoplastid and prokaryotic zeta toxin were downloaded from NCBI protein database. Notably, Ld_ζ1 was found to show a significant proximity to its kinetoplastid family, while the prokaryotic zeta toxin form a distinct separate cluster with high confidence scores as mentioned on the branch nodes (Fig. 1D). To highlight, prokaryotic zeta toxin has been found to cluster with other prokaryotic toxins while Ld_ζ1 was forming discrete clusters with other kinetoplastids, suggesting they share evolutionary relationships (Fig. 1D). Further, the tertiary structure of Ld_ζ1$_{domain}$ was predicted by homology modeling and superimposed with crystal structure of *S. pyogenes* zeta toxin (1GVN.pdb). The superimposed structures showed that the ATP-binding pocket and UNAG cleft are formed by Walker-A and GTXM motif, respectively, resembling prokaryotic zeta toxin (Fig. 1C). Despite the fact that GTXR is replaced by GTXM in kinetoplastids, it could still form the UNAG-binding pocket in predicted structure of Ld_ζ1$_{domain}$. This was also validated *in silico* via possible interaction of Ld_ζ1$_{domain}$ with ATP and UNAG. ATP was found to interact with Walker-A motif of Ld_ζ1$_{domain}$ through four hydrogen bonds that are formed by the residues Lys30, Asn54, Asp56, and Asp96. The binding affinity between ATP and Ld_ζ1$_{domain}$ was -6.4 kcal·mol^{-1}. Similarly, the binding energy of UNAG to Ld_ζ1$_{domain}$ catalytic pocket was -6.9 kcal·mol^{-1} and the predicted residues that form hydrogen bond with UNAG were Asp56 and Thr98 (Fig. 1E). The residues of Ld_ζ1$_{domain}$ involved in hydrogen bond formation are found to be similar with the residues reported for prokaryotic zeta toxin.

Ld_ζ1 possess kinase activity similar to its prokaryotic counterpart

Previous studies states that any protein with a canonical zeta domain possesses UNAG kinase activity [20]. Since predicted structure Ld_ζ1$_{domain}$ has all the conserved motifs stated in prokaryotic zeta toxin, we hypothesized that the predicted Ld_ζ1 protein should also demonstrate the UNAG kinase activity. As a proof of concept, we first overexpressed the 6X-His (at N-terminus) tagged Ld_ζ1$_{domain}$ in *E. coli* and purified it with Ni-NTA resin. The purified recombinant Ld_ζ1$_{domain}$ (rZeta) was detected at ~16 kDa (Fig. 2A). The purified rZeta was used further to evaluate the *in vitro* UNAG kinase activity. This was achieved by using an ADP-Glo™ Kinase assay, which involves ATP regeneration-based luciferase reaction system resulting from nascent ADP phosphorylation. The luminescence signal generated is proportional to the amount of ADP released in the kinase reaction and represents the kinase activity. Different concentrations of rZeta were incubated with its substrates UNAG & ATP, and the optimum kinase activity was observed at 10 μM of rZeta. However, in the absence of UNAG, the rZeta still demonstrated kinase activity (Fig. 2B), strongly indicating autophosphorylation of rZeta. This was further confirmed by Pro-Q Diamond staining which readily detected a band of ~16 kDa corresponding to the molecular weight of rZeta (Fig. 2C). This finding suggested that Ld_ζ1 is the noncanonical kind of zeta toxin demonstrating autophosphorylation property, a characteristic feature of eukaryotic kinases. Most of the eukaryotic protein kinases are regulated or activated by phosphorylation at kinase activation loop. The autophosphorylation activity of Ld_ζ1 may lead to changes in its structural conformation that exposes the substrate-binding domain, thus activating the otherwise inactive Ld_ζ1. Another possibility is that an unrecognized antitoxin might inhibit the autophosphorylation of Ld_ζ1 and regulates its activity.

The optimum temperatures for the growth of promastigotes and amastigotes are 25 °C and 37 °C, respectively. Therefore, the kinase activity of rZeta was tested at both temperatures and the result showed no significant difference in kinase activity at these two temperatures (Fig. 2B).

Previous studies on various bacteria implied that zeta toxins are kinases that phosphorylate the target by binding ATP to canonical Walker-A motif followed

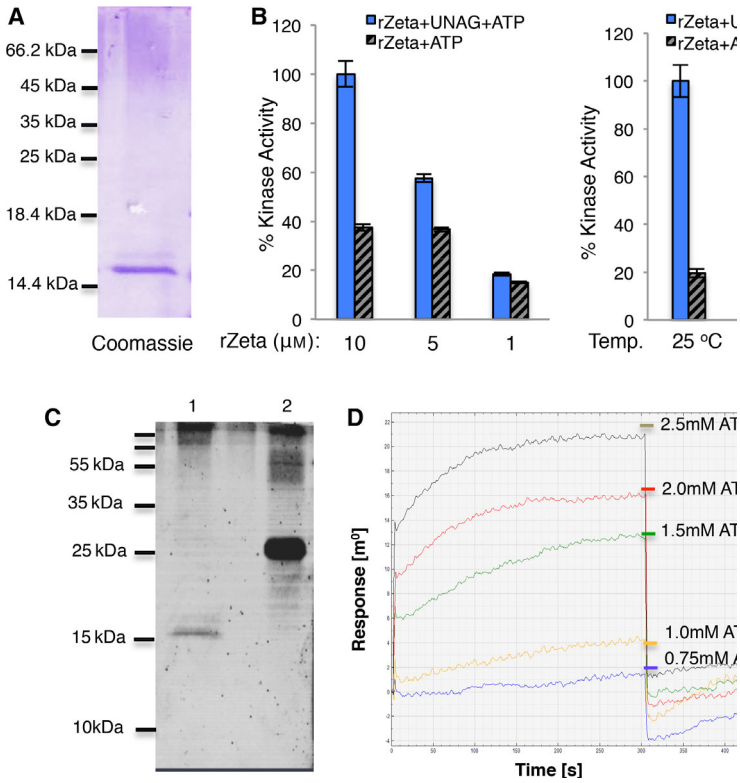

Fig. 2. Ld_ζ1$_{domain}$ hydrolyzes ATP for autophosphorylation and UNAG phosphorylation. (A) His tagged Ld_ζ1$_{domain}$ was purified by Ni-NTA resin and subjected to Coomassie Briliant Blue staining. (B) Different concentrations of purified Ld_ζ1$_{domain}$ were subject to *in vitro* kinase assay in the presence and absence of substrate UNAG. Kinase activity of Ld_ζ1$_{domain}$ was measured at temperatures suitable for promastigote (26 °C) and amastigote (37 °C) as well. (C) Purified Ld_ζ1$_{domain}$ was incubated with ATP and then subjected to Pro-Q Diamond staining to detect autophosphorylation (Lane1: Purified Ld_ζ1$_{domain}$ + ATP; Lane2: phosphorylated caesin as positive control). (D) SPR analysis of ATP interaction to immobilized Ld_ζ1$_{domain}$. Sensorgram of the binding of ATP to Ld_ζ1$_{domain}$ captured on chip at 25 °C.

by its hydrolysis [27,28]. Therefore, to evaluate ATP-mediated phosphorylation by rZeta, we examined the interaction of ATP with rZeta by Surface Plasmon Resonance. Firstly, 6.5 ng of rZeta was immobilized on gold chip and then assessed for its association with ATP. A prominent association curve was observed at and beyond 1.5 mM ATP concentrations (Fig. 2D). Based on these findings, we conclude that the zeta domain of Ld_ζ1 not only phosphorylates its substrate UNAG but also exhibits autophosphorylation property by hydrolyzing ATP. In case of *Leishmania*, UNAG has been used as a precursor in diverse pathways such as, N-linked and O-linked glycans and pathways involving surface expressed GPI anchors [29] but modification of UNAG by phosphorylation has not been reported yet. Therefore, the phosphorylation of UNAG by Ld_ζ1 in *Leishmania* can be predicted to have many effects. Firstly, Ld_ζ1 might play a role in modulating UNAG-based pathway that leads to blockage of surface exposed Glycosylphosphotidylinositol (GPI) biosynthesis. Wanderley *et al.* research states that metacyclic infection to host is enhanced by co-operation between apoptotic and viable metacyclics [30], and thus the role of Ld_ζ1 can be envisaged for generation of these apoptotic promastigotes by blocking the synthesis of the surface exposed GPIs. The second hypothesis might be that when the parasites switch from vector to host or vice versa, it encounters stressed condition that leads to death of certain parasites that might be regulated by the expression of Ld_ζ1. This death might provide the nutrients to the persister parasites, which is in good accordance to the phenomenon reported in bacteria where activation of zeta under stress condition is linked to persistence formation, allowing the bacteria to survive under nutrient deficient conditions [31].

Ld_ζ1 is an active protein in *Leishmania donovani* and might function in growth regulation

Following biochemical characterization of Ld_ζ1, we aimed to confirm the expression of this putative gene at transcriptomic and proteomic level in *L. donovani* promastigote. To achieve the same, cDNA was prepared from *L. donovani* promastigotes and analyzed by RT-PCR. The result clearly showed a band of 175 bp, representing the expression of Ld_ζ1 at transcription level. Amplification was not detected in control having no reverse transcription, thus nullifying DNA contamination present in RNA preparation (Fig. 3A). To further confirm Ld_ζ1 expression at protein level, promastigote parasites were harvested and total protein was extracted using freeze-thaw cycle. The

extracted protein was subjected to immunoblotting using anti- anti-Ld_ζ1$_{domain}$ sera. A band of ~110 kDa corresponding to the expected size of the native parasite protein was detected. Uninduced Ld_ζ1$_{domain}$ *E. coli* lysate was taken as negative control and the recombinant Ld_ζ1$_{domain}$ protein as positive control (Fig. 3B). The expression of active Ld_ζ1 protein was also evaluated by immunofluorescence. When the fixed promastigotes were probed with anti-Ld_ζ1$_{domain}$ sera, staining was observed in vacuole like structure (Fig. 3C). No fluorescence staining was observed with preimmune antibodies confirming the specificity of anti- Ld_ζ1 antibodies (Fig. 3C). As recombinant Ld_ζ1$_{domain}$ was seen to have kinase activity, we speculated that *L. donovani* promastigote lysate should also show kinase activity in the presence of UNAG. To test

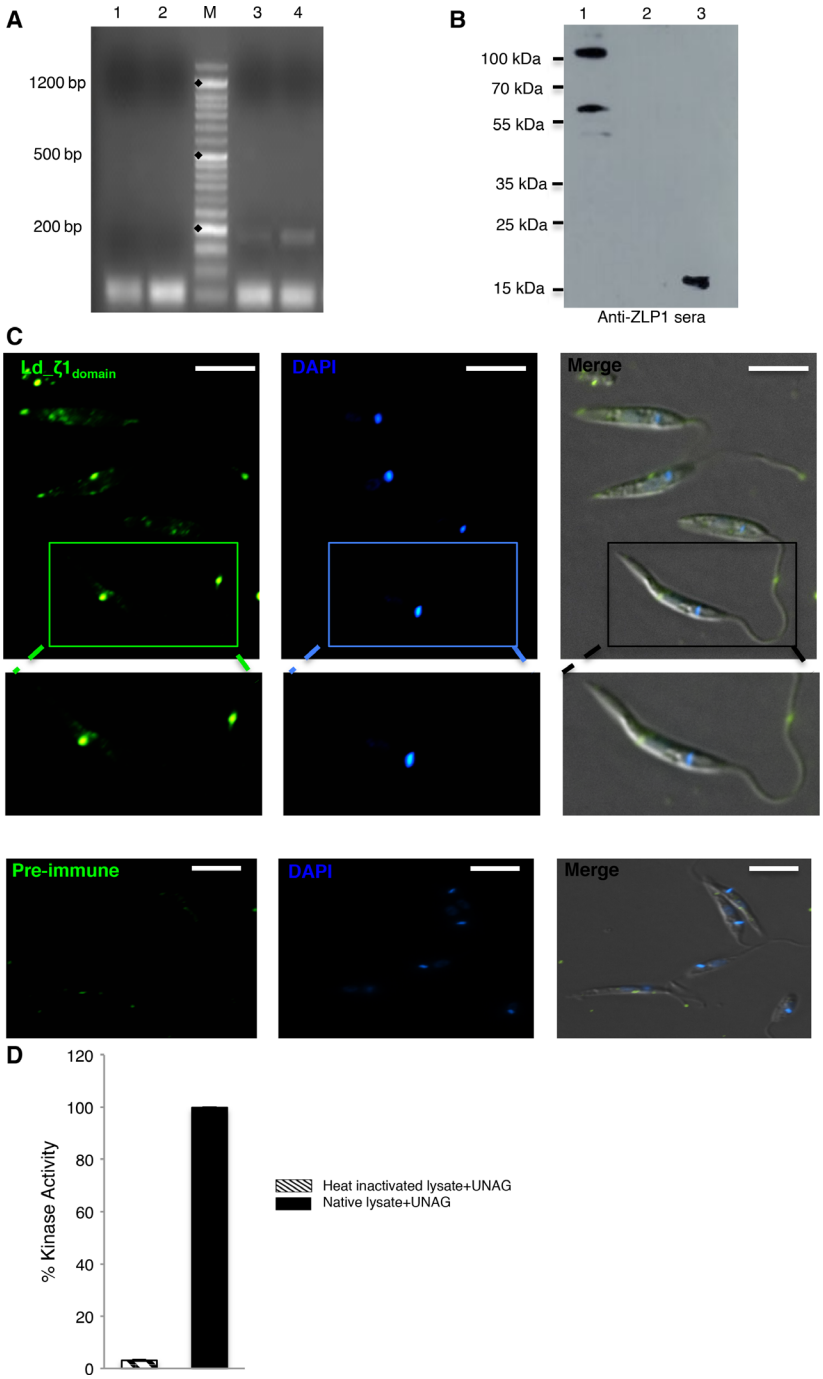

Fig. 3. Ld_ζ1 is expressed in *L. donovani* and exhibits kinase activity. (A) Reverse transcriptase PCR analysis of Ld_ζ1 expression from total RNA of *L. donovani*. The mRNA molecules from stationary phase promastigotes were extracted and analyzed by RT-PCR. Primer used for amplification from cDNA was designed from Ld_ζ1$_{domain}$ region (Lane 1: Without reverse transcriptase as a negative control; Lane 2: No template control; Lane 3: Amplification of Ld_ζ1 at 64 °C; Lane 4: Amplification of Ld_ζ1 at 68 °C). (B) For immunoblotting, anti-Ld_ζ1$_{domain}$ sera raised in mice was used to detect Ld_ζ1 protein in promastigote lysate (Lane 1: *L. donovani* lysate; Lane 2: uninduced *E. coli* lysate expressing Ld_ζ1$_{domain}$; Lane 3: recombinant Ld_ζ1$_{domain}$ protein). (C) Immunofluorescence images represented expression of Ld_ζ1 in fixed promastigotes when probed with anti-Ld_ζ1$_{domain}$ sera raised in mice. Secondary antibody was conjugated with Alexa 488. No staining was detected with preimmune sera. Scale bar represents 10 μm. (D) *In vitro* kinase assay was performed using *L. donovani* lysate as the enzyme source and UNAG (2 mM) as substrate. Heat inactivated lysate was used as negative control.

this possibility, we incubated *L. donovani* lysate (native/heat inactivated enzyme source) with UNAG (substrate) and ATP at 26 °C and proceeded for *in-vitro* kinase assay. Heat inactivated lysate had negligible kinase activity as the proteins of the lysate are in inactive or denatured form. The native lysate demonstrated

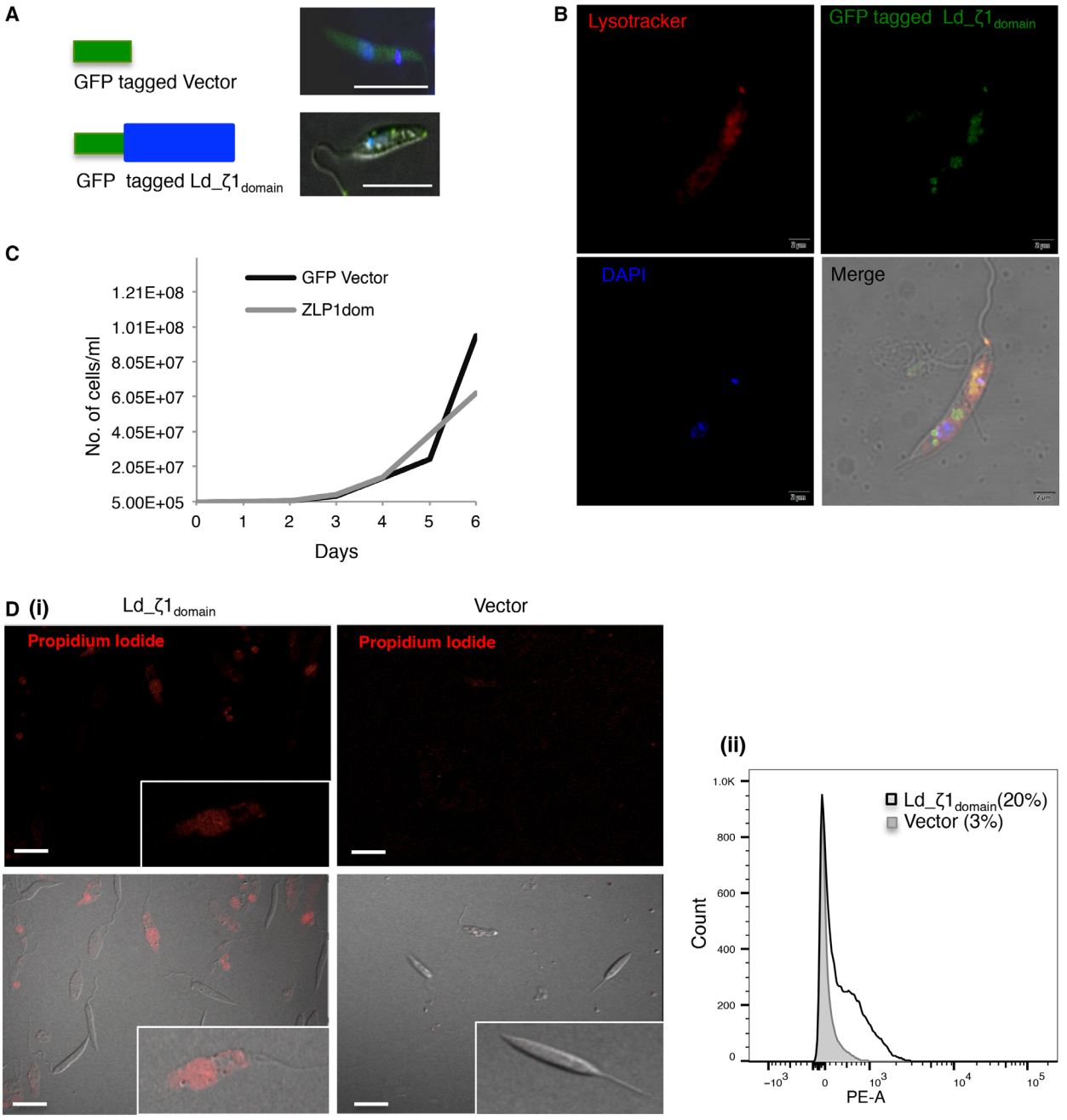

Fig. 4. Ld_ζ1 is toxicity to *L. donovani* is due to membrane permeability. (A) Gene structure of GFP tagged constructs for overexpression in promastigotes. Inset shows GFP fused protein localization in promastigotes. Scale bar represents 10 μm. (B) GFP tagged Ld_ζ1$_{domain}$ overexpressing promastigotes were stained with lysotracker to validate co-localization of protein in acidic organelle-linked with autophagy. Scale bar represents 2 μm. (C) Growth kinetics of promastigotes overexpressing GFP vector and Ld_ζ1$_{domain}$ was measured till Day6. Both the cultures were grown in two parallel vessels with initial count of $5*10^5$ cells·mL^{-1} on Day0. Cells were counted every day till Day6. (D) The influx of membrane impermeable dye Propidium Iodide in promastigotes overexpressing GFP vector and Ld_ζ1$_{domain}$ was measured on Day6 by confocal microscopy (i) and FACS (ii). Scale bar represents 10 μm.

a high kinase activity when supplied with 2 mM UNAG (Fig. 3D).

Furthermore, to decipher subcellular localization and function of Ld_ζ1 protein, we adopted a protein overexpression approach in promastigotes where we overexpressed GFP tagged Ld_ζ1$_{domain}$ and GFP vector in *L. donovani* promastigotes. The localization of Ld_ζ1$_{domain}$ was observed as GFP fluorescence in vacuole like structure, whereas GFP fluorescence for vector control was dispersed throughout the cytosol (Fig. 4A). Additionally, the co-localization of Ld_ζ1 was studied by staining with lysotracker, a dye that stains acidic organelles. Co-staining of GFP fluorescence of Ld_ζ1 with lysotracker validates that Ld_ζ1 is located in vacuole like structure associated with programmed cell death (Fig. 4B). This was consistent with the immunofluorescence observation for Ld_ζ1 staining.

Prokaryotic zeta toxins are known to mediate reversible protective dormancy and permeation to propidium iodide (PI) [32]. Therefore, to evaluate whether the Ld_ζ1 protein is correlated with programmed cell death due to toxicity in *L. donovani*, we examined the growth kinetics of promastigotes overexpressing Ld_ζ1$_{domain}$ and vector. During the early log phase, the growth pattern for promastigotes overexpressing Ld_ζ1$_{domain}$ and vector did not show any significant difference but a decrease in growth during exponential phase was noticed in Ld_ζ1$_{domain}$ overexpressing promastigotes (Fig. 4C). Next, we investigated if Ld_ζ1$_{domain}$ -mediated growth reduction is attributed to cell death caused by a defect in the cell wall as was previously reported for bacterial zeta toxin. To achieve this, we stained the Ld_ζ1$_{domain}$ overexpressing promastigotes with PI and analyzed through FACS. We found that PI influx in promastigotes overexpressing Ld_ζ1$_{domain}$ was enhanced when compared to vector control and hence is indicative of loss of phosphoglycan membrane integrity. Confocal imaging of PI^{pos} promastigotes further confirmed the influx of PI in promastigotes. Notably, the shape of PI^{pos} promastigotes was disrupted as compared to PI^{neg} promastigotes that exhibited classical highly elongated morphology (Fig. 4D). Overall, the phenotypic observation in promastigotes overexpressing Ld_ζ1domain indicated the predominant existence of zeta toxin like proteins, which is coherent with the prokaryotic zeta toxin.

Heterologous expression of Ld_ζ1$_{domain}$ in *Escherichia coli* results in cell toxicity due to Ld_ζ1$_{domain}$ kinase activity

E. coli is a proven and well-established model system for characterization of the functional activity of various zeta toxins [20]. Therefore, for phenotypic characterization of eukaryotic Ld_ζ1, we used *E. coli* as a heterologous model system. A study conducted by Rocker and Meinhart [8] showed that zeta toxin of *E. coli* is more active below ambient temperature (<30 °C) in order to regulate bacterial survival outside the host [8]. In concordance with this finding, we tried to observe the effect of overexpression of Ld_ζ1 on the growth of *E. coli* at different temperatures. At 37 °C, less cytotoxicity of Ld_ζ1$_{domain}$ with 1.2-fold bacterial growth restriction was observed in the induced sample, as compared to uninduced sample. In contrast, at 25 °C 2.5-fold growth restriction was obtained. Further decreasing the growth temperature to 18 °C resulted in dormant state or cell growth arrest in Ld_ζ1$_{domain}$ overexpressing *E. coli* cells with a 9-fold difference in cell growth kinetics (Fig. 5A). This cell proliferation arrest reverted back when toxin-induced cells were incubated back to 37 °C and partly regained its normal morphology. It is likely that toxin Ld_ζ1$_{domain}$ might halt cell proliferation as an outcome of protective response as earlier explained by Lioy *et al.* [21], Mutschler *et al.* [33]. We also noted that with increasing time of expression of Ld_ζ1$_{domain}$ at 18 °C, *E. coli* cells displayed more membrane permeability, evident by influx of the membrane-impermeable dye propidium iodide (Fig. 5B). Eventually, this phenotype of *E. coli* is due to the compromised cell wall, which strongly aligns with results from previous

Fig. 5. Ld_ζ1$_{domain}$ toxicity in heterologous *E. coli* system is specific to its kinase activity and similar to its prokaryotic counterpart. (A) Growth kinetics of *E. coli* cells expressing Ld_ζ1$_{domain}$ was monitored at different temperatures by measuring the optical density (O.D.) of cultures. Growth kinetics was measured with respect to time. Cells were induced at 0.07 O.D. with 1 mM IPTG and incubated at respective temperature. (B) Phase contrast and fluorescence microscopy (live-dead staining) images of *E. coli* cells overexpressing Ld_ζ1$_{domain}$ post-8 h and 12 h of induction at 18 °C. Blue fluorescence of cells indicate live cells with intact cell membrane. Influx of propidium iodide (red fluorescence) is due to membrane permeability. Scale bar represents 10 μm. (C) Effect on growth of *E. coli* cells overexpressing Ld_ζ1$_{domain}$ was measured in the presence of exogenously supplied UNAG in uninduced and toxin-induced samples at 18 °C. UNAG was added at the time of induction. Colony forming unit assay was performed to determine cell growth. The experiment was performed thrice. Bacterial CFU graph is 4 h postinduction at 10^{-6} dilution. *Note: For CFU assay, different dilutions were prepared at desired time point and then 5 μL was plated from each dilution.

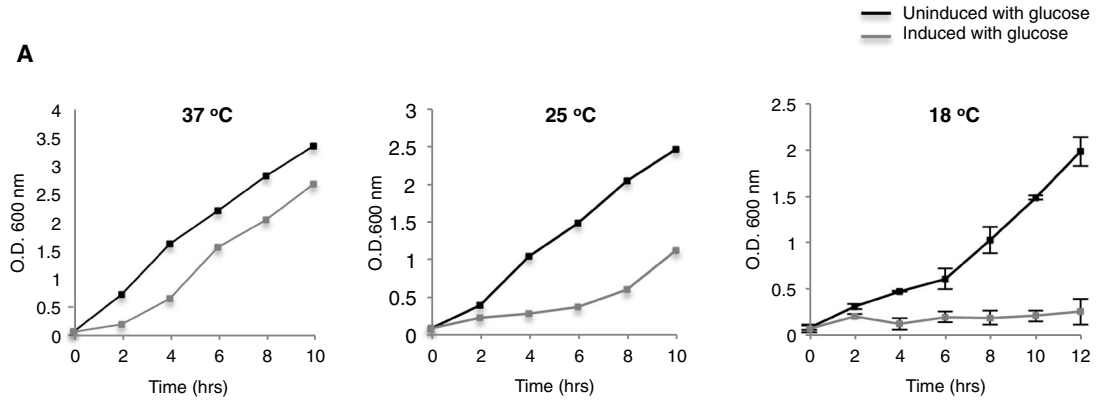

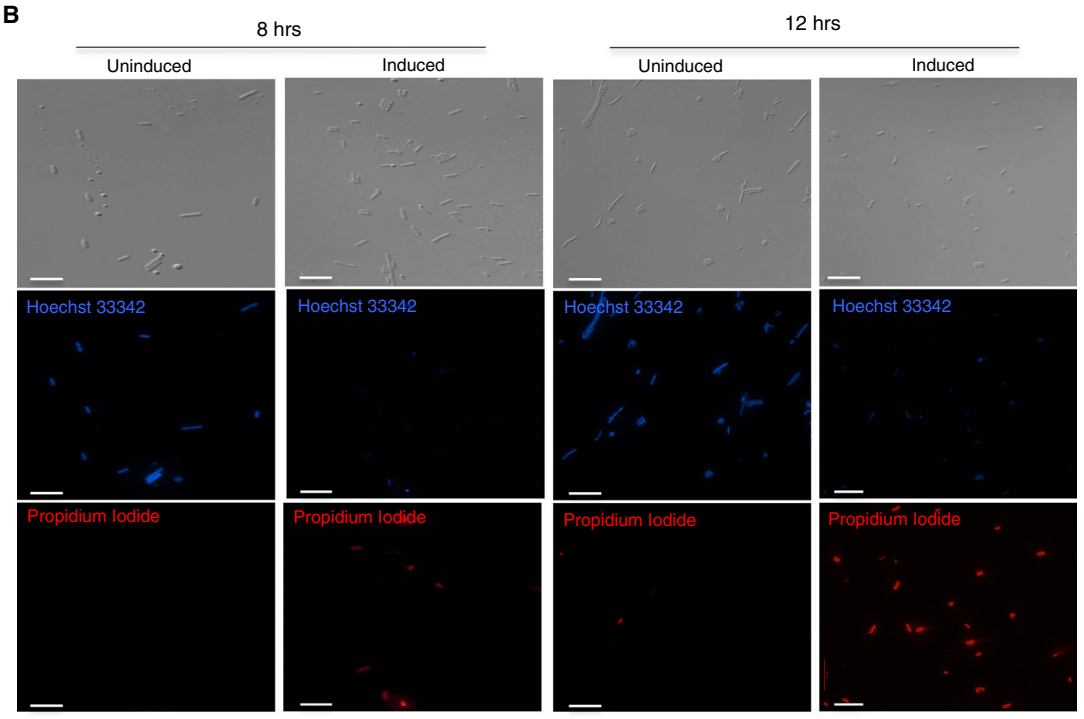

C

Experimental Conditions	4 hrs				8 hrs			
	10^{-1}	10^{-3}	10^{-5}	10^{-6}	10^{-1}	10^{-3}	10^{-5}	10^{-6}
Uninduced sample								
Induced sample								
Induced sample with 2mM UNAG								

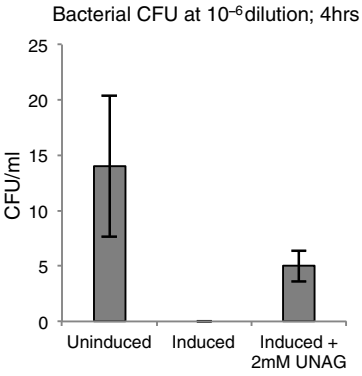

phenotypic analysis of prokaryotic zeta toxin [21,20]. Thus, our data illustrates that Ld_ζ1$_{domain}$ toxicity is temperature-dependent with pronounced activity at lower temperatures, which further induces cell dormancy.

Uridine diphosphate N-acetyl glucosamine is an essential metabolite involved in bacterial cell wall synthesis pathway and, it is noteworthy that phosphorylation of UNAG by zeta toxin results in impaired cell wall synthesis [20]. We speculated that if the toxicity of *E. coli* cells overexpressing Ld_ζ1$_{domain}$ is due to unavailability of UNAG that leads to inhibition of peptidoglycan synthesis pathway, then providing excess of UNAG must rescue the total cell population undergoing dormancy or lysis. Toward this, we supplied 2 mM of UNAG in culture at the time of toxin-induction and the result suggested a remarkable increase in the number of colonies measured through the colony forming unit (CFU) assay (Fig. 5C). The increase in the number of colonies when exogenous UNAG was supplied in culture induced with Ld_ζ1$_{domain}$ was statistically significant over the Ld_ζ1$_{domain}$ induced culture that was not supplied with UNAG. These cumulative results demonstrates that the growth reduction in Ld_ζ1$_{domain}$ overproducing cells is due to the kinase activity of the zeta domain and has a direct or indirect effect on the cell wall, as excess substrate reverses the cell wall damage by allowing the cells to divide.

The results obtained by overproducing Ld_ζ1$_{domain}$ in *E. coli* is in good agreement with our observation obtained by overexpressing Ld_ζ1$_{domain}$ in promastigotes and a previous report that showed a toxic effect of bacterial zeta toxin when overexpressed in a eukaryote (*S. cervisiae*) [34]. Taken together, this study suggests that the modification of UNAG by zeta toxin damages a shared pathway that is present both in prokaryotes and eukaryotes. However, for a more thorough understanding and specific function of this gene, the generation of Ld_ζ1 knock out will provide a deeper insight into its mechanism. Overall, we report for the first time, a zeta toxin like protein in a eukaryotic parasite, *L. donovani,* which has UNAG kinase activity similar to conventional zeta toxins along with the unique autophosphorylation activity.

Acknowledgements

This work was supported by an extramural research grant (EMR/2016/005644) from Science & Engineering Research Board (SERB), Department of Science & Technology, which was awarded to SS. AS and RA are supported by the Shiv Nadar Foundation fellowship, Shiv Nadar University. RJ is supported by UGC-JRF fellowship. SG is thankful for the funding support from DST-INSPIRE grant. SP is grateful for the funding support from Shiv Nadar foundation. Authors acknowledge Surface Plasma Resonance facility of AIRF, Jawaharlal Nehru University (JNU) and central facility of Special Centre for Molecular Medicine (SCMM), JNU for flow cytometer.

Author contributions

SS and SG conceptualized and designed the study. AS performed cloning, expression and characterization of proteins and compiled the data. AS and RJ performed kinase assay. RA and SP have performed *in silico* docking. AS and HK have generated antibody in mice and performed domain purification. AS and LG has analyzed the protein purification data. AS and SP have written the manuscript. SS has corrected and approved the final draft.

References

1 Kima PE (2007) The amastigote forms of *Leishmania* are experts at exploiting host cell processes to establish infection and persist. *Int J Parasitol* **37**, 1087–1096.
2 Oryan A and Akbari M (2016) Worldwide risk factors in leishmaniasis. *Asian Pacific J Trop Med* **9**, 925–932.
3 Cota GF, De Sousa MR and Rabello A (2011) Predictors of visceral leishmaniasis relapse in HIV-infected patients: a systematic review. *PLoS Negl Trop Dis* **5**, e1153.
4 Guerin PJ, Olliaro P, Sundar S, Boelaert M, Croft SL, Desjeux P, Wasunna MK and Bryceson AD (2002) VisceraAl leishmaniasis: current status of control, diagnosis, and treatement, and a proposed research and development agenda. *Lancet Infect Dis* **2**, 494–501.
5 Croft SL, Sundar S and Fairlamb AH (2006) Drug resistance in leishmaniasis. *Clin Microbiol Rev* **19**, 111–126.
6 Downing T, Imamura H, Decuypere S, Clark TG, Coombs GH, Cotton JA, Hilley JD, de Doncker S, Maes I, Mottram JC *et al.* (2011) Whole genome sequencing of multiple *Leishmania donovani* clinical isolates provides insights into population structure and mechanisms of drug resistance. *Genome Res* **21**, 2143–2156.
7 Worthey EA, Martinez-Calvillo S, Schnaufer A, Aggarwal G, Cawthra J, Fazelinia G, Fong C, Fu G, Hassebrock M, Hixson G *et al.* (2003) Leishmania major chromosome 3 contains two long convergent polycistronic gene clusters separated by a tRNA gene. *Nucleic Acids Res* **31**, 4201–4210.
8 Rocker A and Meinhart A (2015) A cis-acting antitoxin domain within the chromosomal toxin–antitoxin module

EzeT of *Escherichia coli* quenches toxin activity. *Mol Microbiol* **97**, 589–604.
9 Unterholzner JS, Poppenberger B and Rozhon W (2013) Toxin–antitoxin systems biology, identification, and application. *Mob Genet Elements* **3**, e26219.
10 Ghafourian S, Raftari M, Sadeghifard N and Sekawi Z (2014) Toxin-antitoxin systems: classification, biological function and application in Biotechnology. *Curr Issues Mol Biol* **16**, 9–14.
11 Jurenaite M, Markuckas A and Suziedeliene E (2013) Identification and characterization of type II toxin-antitoxin systems in the opportunistic pathogen *Acinetobacter baumannii*. *J Bacteriol* **195**, 3165–3172.
12 Brantl S and Jahn N (2015) sRNAs in bacterial type I and type III toxin-antitoxin systems. *FEMS Microbiol Rev* **39**, 413–427.
13 Page R and Peti W (2016) Toxin-antitoxin systems in bacterial growth arrest and persistence. *Nat Chem Biol* **12**, 20814.
14 Schuster CF and Bertram R (2013) Toxin-antitoxin systems are ubiquitous and versatile modulators of prokaryotic cell fate. *FEMS Microbiol Lett* **340**, 73–85.
15 Leplae R, Geeraerts D, Hallez R, Guglielmini J, Dreze P and Van Melderen L (2011) Diversity of bacterial type II toxin-antitoxin systems: a comprehensive search and functional analysis of novel families. *Nucleic Acids Res* **39**, 5513–5525.
16 Meinhart A, Alonso JC, Strater N and Saenger W (2003) Crystal structure of the plasmid maintenance system epsilon/zeta: functional mechanism of toxin zeta and inactivation by epsilon 2 zeta 2 complex formation. *Proc Natl Acad Sci USA* **100**, 1661–1666.
17 Saraste M, Sibbald PR and Wittinghofer A (1990) The P-loop–a common motif in ATP- and GTP-binding proteins. *Trends Biochem Sci* **15**, 430–434.
18 Barreteau H, Kovac A, Boniface A, Sova M, Gobec S and Blanot D (2008) Cytoplasmic steps of peptidoglycan biosynthesis. *FEMS Microbiol Rev* **32**, 168–207.
19 El Zoeiby A, Sanschagrin F and Levesque RC (2003) Structure and function of the Mur enzymes: development of novel inhibitors. *Mol Microbiol* **47**, 1–12.
20 Mutschler H, Gebhardt M, Shoeman RL and Meinhart A (2011) A novel mechanism of programmed cell death in bacteria by toxin–antitoxin systems corrupts peptidoglycan synthesis. *PLoS Biol* **9**, e1001033.
21 Lioy VS, Martin MT, Camacho AG, Lurz R, Antelmann H, Heker M, Hitchin E, Ridge Y, Wells JM and Alonso JC (2006) pSM19035-encoded zeta toxin induces stasis followed by death in a subpopulation of cells. *Microbiology* **152**, 2365–2379.
22 Zielenkiewicz U and Ceglowski P (2005) The toxin-antitoxin system of the streptococcal plasmid pSM19035. *J Bacteriol* **187**, 6094–6105.
23 Rocker A, Peschke M, Kittilä T, Sakson R, Brieke C and Meinhart A (2018) The ng_ζ1 toxin of the gonococcal epsilon/zeta toxin/antitoxin system drains precursors for cell wall synthesis. *Nat Commun* **9**, 1686.
24 Vallur AC, Tutterrow YL, Mohamath R, Pattabhi S, Hailu A, Abdoun AO, Ahmed AE, Mukhtar M, Salam MA, Almeida ML *et al.* (2015) Development and comparative evaluation of two antigen detection tests for Visceral Leishmaniasis. *BMC Infect Dis* **15**, 384.
25 Ayana R, Yadav P, Kumari R, Ramu D, Garg S, Pati S and Singh S (2018) Identification and characterization of a novel Palmitoyl Acyltransferase as a Druggable Rheostat of dynamic Palmitoylome in *L. donovani*. *Front Cell Infect Microbiol* **8**, 186.
26 Mutschler H and Meinhart A (2011) ε/ζ systems: their role in resistance, virulence, and their potential for antibiotic development. *J Mol Med* **89** (12), 1183–1194.
27 Khoo SK, Loll B, Chan WT, Shoeman RL, Ngoo L, Yeo CC and Meinhart A (2007) Molecular and structural characterization of the PezAT chromosomal toxin–antitoxin system of the human pathogen *Streptococcus pneumoniae*. *J Biol Chem* **282**, 19606–19618.
28 Nowakowska B, Kern-Zdanowicz I, Zielenkiewicz U and Ceglowski P (2005) Characterization of *Bacillus subtilis* clones surviving overproduction of Zeta, a pSM19035 plasmid-encoded toxin. *Acta Biochim Pol* **52**, 99–107.
29 Naderer T, Wee E and McConville MJ (2008) Role of hexosamine biosynthesis in Leishmania growth and virulence. *Mol Microbiol* **69**, 858–869.
30 Wanderley JLM, Pinto da Silva LH, Deolindo P, Soong L, Borges VM, Prates DB, Almeida de Souza AP, Barral A, Balanco JMF, Nascimento MTC *et al.* (2009) Cooperation between apoptotic and viable metacyclics enhances the pathogenesis of Leishmaniasis. *PLoS ONE* **4**, e5733.
31 Moreno-Del Álamo M, Tabone M, Lioy VS and Alonso JC (2017) Toxin ζ triggers a survival response to cope with stress and persistence. *Front Microbiol* **8**, 1130.
32 Lioy VS, Machon C, Tabone M, Gonzalez-Pastor JE, Daugelavicius R, Ayora S and Alonso JC (2012) The ζ toxin induces a set of protective responses and dormancy. *PLoS ONE* **7** (1), e30282.
33 Mutschler H, Reinstein J and Meinhart A (2010) Assembly dynamics and stability of the pneumococcal Epsilon Zeta antitoxin toxin (PezAT) system from *Streptococcus pneumoniae*. *J Biol Chem* **285**, 21797–21806.
34 Zielenkiewicz U, Kowalewska M, Kaczor C and Ceglowski P (2009) In vivo interactions between toxin-antitoxin proteins epsilon and zeta of streptococcal plasmid pSM19035 in *Saccharomyces cerevisiae*. *J Bacteriol* **191**, 3677–3684.